Vol 16 No 8, August 2007
1009-1963/2007/16(08)/2455-07

Chinese Physics

© 2007 Chin. Phys. Soc.
and IOP Publishing Ltd

Dopant diffusion and surface morphology of vanadium implanted 4H-silicon carbide*

Wang Chao(王 超)†, Zhang Yi-Men(张义门), Zhang Yu-Ming(张玉明),
Ma Ge-Lin(马格林), Guo Hui(郭 辉), and Xu Da-Qing(徐大庆)

Institute of Microelectronics, Xidian University,

Key Laboratory of Ministry of Education for Wide Band-Gap Semiconductor Materials and Devices, Xi'an 710071, *China*

(Received 20 December 2006; revised manuscript received 16 January 2007)

The diffusion behaviours of vanadium implanted p- and n-type 4H-SiC are investigated by using the secondary ion mass spectrometry (SIMS). Significant redistribution, especially out-diffusion of vanadium towards the sample surface is not observed after 1650 °C annealing for both p- and n-type samples. Atomic force microscopy (AFM) is applied to the characterization of surface morphology, indicating the formation of continuous long furrows running in one direction across the wafer surface after 1650 °C annealing. The surface roughness results from the evaporation and re-deposition of Si species on the surface during annealing. The chemical compositions of sample surface are investigated using x-ray photoelectron spectroscopy (XPS). The results of C 1s and Si 2p core-level spectra are presented in detail to demonstrate the evaporation of Si from the wafer and the deposition of SiO_2 on the sample surface during annealing.

Keywords: vanadium implanted SiC, annealing, diffusion, surface morphology
PACC: 6170T, 6170W, 6822, 3365F

1. Introduction

Silicon carbide is currently being explored as a promising wide band gap semiconductor for high-temperature, high-frequency, and high-power devices. Ion implantation is an important technique of SiC technology for doping; for example, aluminium, boron and nitrogen have been studied intensively for p-type and n-type doping[1,2]. Moreover, there are also numerous researches on electrical isolation by using this technique, and vanadium ions, known to be able to generate deep levels to trap the carriers, have achieved a great success in the formation of high-resistive region in SiC.[3−5] In our early works, the resistivities have reached as high as $10^{10}\Omega$ cm and $10^6\,\Omega$ cm respectively for V-implanted p- and n-type 4H-SiC samples at room temperature.[6,7] The compensation for isolation by implantation is highly desirable over mesa etching mainly due to planarity concerns. For manufacturing processes, such as lithography, planarity of the devices is desirable for high-density integration.

Post-implantation annealing is necessary to electrically activate dopants. Higher resistivity can be obtained by annealing at temperatures of above 1600 °C to electrically activate more vanadium ions for compensation.[7,8] However, high-temperature annealing results in the diffusion of dopants in SiC. For example, the shape of beryllium implanted profile in SiC is considerably changed after annealing.[9] Depletion of V near the surface region due to out-diffusion is not desirable because it results in low resistivity for lack of the compensation. If this occurs, achieving better inter-device isolation will not be possible.

An additional problem inherent to SiC is the degradation of the surface morphology during high temperature annealing. The surface roughness is known as furrow like structures due to the 'step bunching' effect caused by the incongruent evaporation of Si from the SiC wafer and the re-deposition of SiC species on the surface during annealing.[10,11] The re-deposited SiC species initially assumed to be Si, Si_2C, SiC_2, etc. by Capano *et al.*[11] But these species have not yet been found experimentally.

In this work, the SIMS measurements are performed on as-implanted and post-implantation annealed samples to investigate the distribution of vanadium in SiC before and after high temperature an-

*Project supported by the National Natural Science Foundation of China (Grant No 60376001), the National Basic Research Program of China (Grant No 2002CB311904) and the National Defense Basic Research Program of China (Grant No 51327020202).
†Corresponding author. E-mail: chwang@mail.xidian.edu.cn

nealing. The sample morphologies are characterized by AFM. The physical characteristics of SiC samples before and after annealing are investigated by XPS.

2. Experimental details

Experiments are performed separately on a 4.9 μm thick p-type ($N_a = 1.0 \times 10^{16}$ cm^{-3}) and n-type ($N_d = 5.2 \times 10^{15}$ cm^{-3}) 4H-SiC epitaxial layer grown on Si face, (0001) oriented (8° off), n-doped substrate from Cree Research, Inc. After proper cleaning, V ions are implanted with a 1.4×10^{13} cm^{-2} dose at 2100 keV. Ion range distributions are obtained by Monte Carlo simulations using the TRIM code and then checked by SIMS. Post-implantation annealing is performed in argon atmosphere at 1650 °C for 30 min.

V depth profiles are analysed by SIMS using a CAMECA-ims-4f instrument with a 10.5 keV O_2^+ primary ion beam. A primary beam current of 1 μA is focused and rastered over an area of 250 μm×250 μm. The secondary ion signal is extracted from a 60 μm diameter circular area centred in the rastered region. The depth scales are determined by measuring the total crater depth with a surface profiler and assuming a constant sputtering rate during depth profiling. The concentration scales are determined by assuming that the stated nominal implantation fluence is correct.

The surface morphology of SiC samples before and after annealing is characterized by AFM using a SHIMADZU SPM-9500J3 instrument. The AFM is performed on a 10 μm×10μm square at a scan rate of 1–10Hz in air at atmospheric pressure inside a vibration isolation chamber.

The study of the composition and properties of samples before and after annealing is performed using XPS. The XPS spectra are obtained using a KRATOS AXIS ULTRA spectrometer with a monochromatic Al $K\alpha$ radiation (1486.6 eV) operated at a power of 150 W (15 kV and 10 mA). The vacuum in the spectrometer is 1.3×10^{-7} Pa during measurements. Binding energies are calibrated relative to the C ls peak (284.8 eV) from C–C bonds of the samples.

3. Results and discussion

3.1. SIMS results

The SIMS depth profiles of V in the V-implanted samples before and after annealing are shown in Fig.1. For the as-implanted profiles in p- and n-type 4H-SiC, the concentration tail near the surface and the mean concentration are well reproduced by the Monte Carlo simulation (see Figs.1(a) and 1(b)). However, the tail in the bulk of the epilayer extends to regions deeper than those of the simulated profiles for V-implanted p- and n-type samples, respectively. Channelling effects, which are not considered in TRIM, are assumed to be responsible for the observed discrepancy.[9]

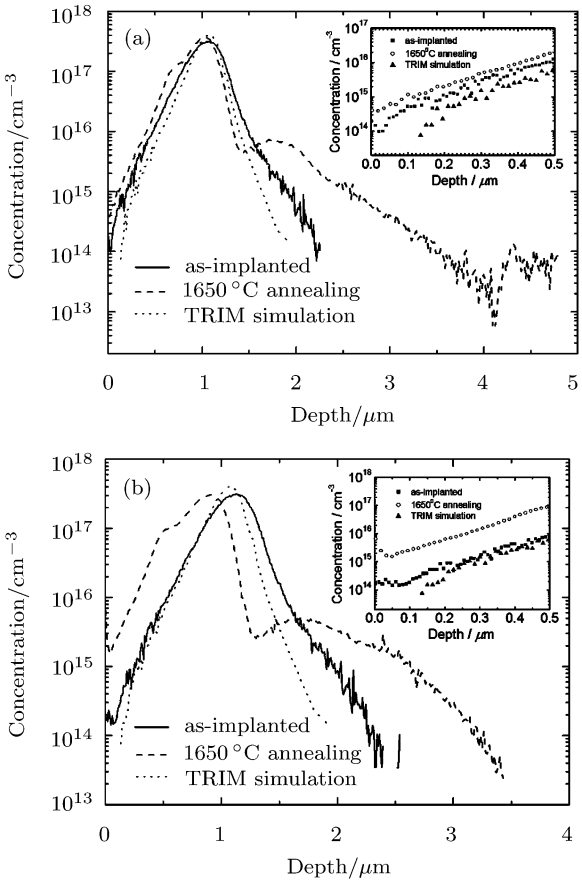


Fig.1. SIMS depth profiles for V-implanted p-type (a), and n-type 4H-SiC (b). The inset clearly shows the distribution of vanadium ions near the sample surface.

The concentration tail near the surface and the mean concentration in 1650 °C annealed samples are equal to those in as-implanted samples for V-implanted p-type SiC (see Fig.1(a)), which indicates that V shows little out-diffusion behaviour during annealing. Whereas, a little in-diffusion tail extending to a deeper region is observed after 1650 °C annealing. The V atoms do not show to have a significant in-diffusion rate but show to have a relatively low out-diffusion rate in n-type sample after annealing (see Fig.1(b)). A slight shift of the peak of implanted V concentration towards the surface can be seen.

An out-diffusion of vanadium towards the surface can be better visualized in the inset. The surface pile-up is not observed in Fig.1(a). A slight pile-up of vanadium in the surface layer appears in Fig.1(b), but it is not pronounced. A strong surface pile-up is due to the significant out-diffusion of dopants. SIMS measurements reveal that V shows an insignificant out-diffusion behaviour in annealed p- and n-type samples. This means that the depletion of V atoms near the surface region does not occur for p- and n-type 4H-SiC samples, separately.

The transition metals diffuse by the interstitial-substitutional diffusion mechanism in Si.[12] Their behaviours in SiC are not known. Compared with III–V compounds, the transition metals are relatively stable in SiC. Significant redistribution is not observed after 1650 °C annealing for p- and n-type samples, and the out-diffusion of vanadium towards the surface is not observed. In particular, V in p-type SiC samples is stable compared with in n-type samples during high temperature annealing.

3.2. Surface morphology of SiC samples

A series of AFM results in Fig.2 reveals the surface morphology of vanadium-implanted 4H-SiC before and after annealing. From Figs.2(a) and 2(b), the surface roughness is not seen after ion implantation. The continuous long furrows (undulation) running in one direction across the wafer surface are observed after annealing in Figs.2(c) and 2(d). This observation is independent of whether the sample is p-type or n-type 4H-SiC. The degree of roughness in the annealed n-type sample is more than that in the annealed p-type sample. For the annealed n-type sample, the pitch between peaks of the furrows decreases, and depth of the grooves increases. This may be due to the difference in initial conduction type and dopants concentration between p- and n-type 4H-SiC samples. But there has been no report about these phenomena so far. Detailed experiments and analysis are required to be performed in the future.

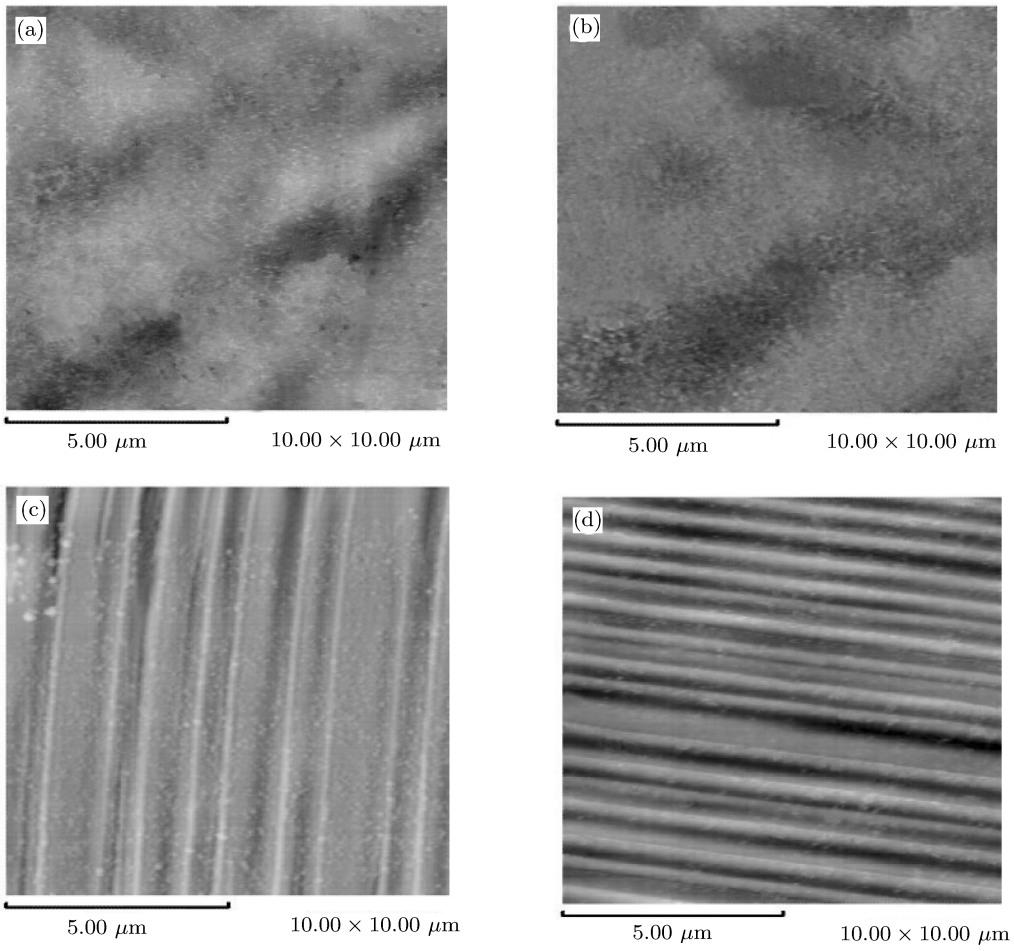


Fig.2. AFM results obtained for 4H-SiC samples: (a) as received, (b) vanadium implanted, (c) vanadium implanted p-type and annealed, and (d) vanadium implanted n-type and annealed.

The out-diffusion of implanted ions is more prominent with the degree of surface roughness increasing.[13] That is why the out-diffusion of vanadium ions in n-type samples is a little more than that in p-type samples during annealing as discussed above. Values for the root-mean-square (RMS) roughness and furrow spacing are listed in Table 1.

A model has been proposed to explain the observed surface roughness.[11] An initial assumption of this model is that the post-implanted, un-annealed sample surface is characterized by a uniform array of 1.0 nm steps for 4H-SiC, which is produced during epitaxy. This assumption is justified based on the statistical analysis of step heights performed by Kimoto *et al*[14] and the RMS roughness data from Table 1. A schematic illustration of a 4H-SiC surface prior to annealing is presented in Fig.3(a).

Table 1. RMS roughness and furrow spacing for 4H-SiC.

	As received	As implanted	Annealed p-type	Annealed n-type
Roughness/nm	0.7	0.8	5.6	7.9
Spacing/nm	n/a^*	n/a^*	860	567

*Not available: roughness not developed sufficiently to provide meaningful results.

Annealing at high temperatures, while providing the driving force required to activate implanted dopants for diffusion-based processes, also permits the surface to approach its equilibrium form. The proposed equilibrium morphology is presented in Fig.3(b), which comprises large basal-plane terraces. The total surface area represented by Fig.3(b) is equivalent to that represented by Fig.3(a). There is no surface area (energy) penalty associated with the transformation from a structure represented by Fig.3(a) into that represented by Fig.3(b). It must be realized that the step edges are locations where the dangling bond density is high, which is energetically unfavourable. Consequently, a net reduction in free energy is realized as the surface evolves from Fig.3(a) to Fig.3(b).

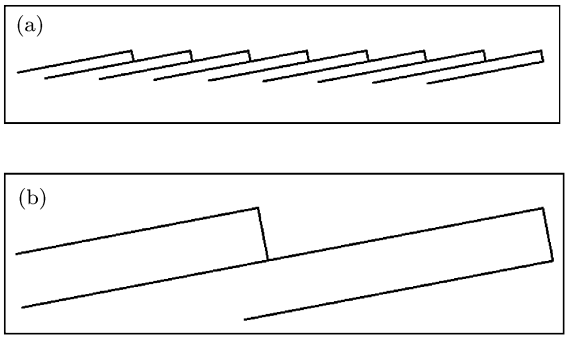


Fig.3. Cross-sectional illustration of SiC surface morphology. Each step in (a) represents the stacking of four Si-C bilayers, which are formed during epitaxy of 4H-SiC. Steps in (b) represent the stacking of many bilayers, and the surface transforms into this equilibrium form during high temperature annealing in argon.

A mechanistic description of this morphological transformation is not yet available, but the data and the experimental procedures suggest feasible pathways.[10,11] The process must be initiated by the dissociation of SiC, leading to the desorption of Si-containing molecules from SiC (sublimation), and the accumulation of mobile species on the surface. Step bunching,[15] which traditionally means that the bunching occurs during epitaxy and all steps flow in the down-step direction (to the right in Fig.3(a)), cannot give rise to the observed roughness because there is a net accumulation of SiC for such an occurrence but no external Si or C source needed for growth. It is likely that a dynamic step flow process during sublimation contributes to the step bunching and the formation of macrosteps as seen in Figs.2(c) and 2(d). That is, sublimation takes place by the sequential removal of monolayers resulting from desorption at step edges; this coordinated flow of steps in a direction opposite to that for epitaxy can lead to the step bunching, because bilayers in the unit cell each have a surface energy different from the others and it is this surface energy anisotropy that leads to bunching.[16]

However, this mechanism is just one of several thermally activated events occurring on the SiC surface as it dissociates. The desorption at step edges and the re-deposition of mobile Si-containing species on the SiC surface take place during high temperature treatment. All of these are considered to be involved in the surface transformation process. The latter is thought to originate from the step edges and from the molecular species that are desorbed and recondense onto the surface. The surface is reconfigured itself into an equilibrium form during annealing, which includes macrosteps, through sublimation and the accumulation of mobile species on the SiC surface. In the

regions where the accumulation on the surface takes place, the step flow in the down-step direction (similar to that for epitaxy) occurs. When the surface is viewed as a whole, a dynamic situation is established where positive (growth) and negative (desorption), localized desorption from terraces, and re-deposition of mobile species are all combined to convert the surface into a new configuration that resembles the equilibrium state illustrated in Fig.3(b).

The cross-sectional representation in Fig.3(b) appears as furrows extend in one direction, which can be seen by viewing from the above the surface. The similarity between this illustration and the images of Figs.2(c) and 2(d) supports the model. It is obvious that the annealing conditions are required to attain high activation against maintaining planar surfaces, unless SiC sublimation is suppressed. Recent experiments demonstrate that the AlN encapsulation,[17] the carbon cap[18] and a silane overpressure[19] can all effectively reduce the surface degradation during annealing.

3.3. XPS analysis

To explain the phenomena observed in the AFM experiments, the detailed investigation of the chemical compositions due to annealing is important. Hence XPS spectra are measured for the implanted samples before and after annealing. The concentrations of C and Si atoms before and after annealing are listed in Table 2.

Table 2. C and Si atomic concentrations in V-implanted 4H-SiC samples before and after annealing.

Atomic concentration	V-implanted p-type SiC		V-implanted n-type SiC	
	un-annealed	annealed	un-annealed	annealed
C/%	51.17	46.27	52.75	42.54
Si/%	48.83	53.73	47.25	57.46
Ratio of C to Si	1.05	0.86	1.12	0.74

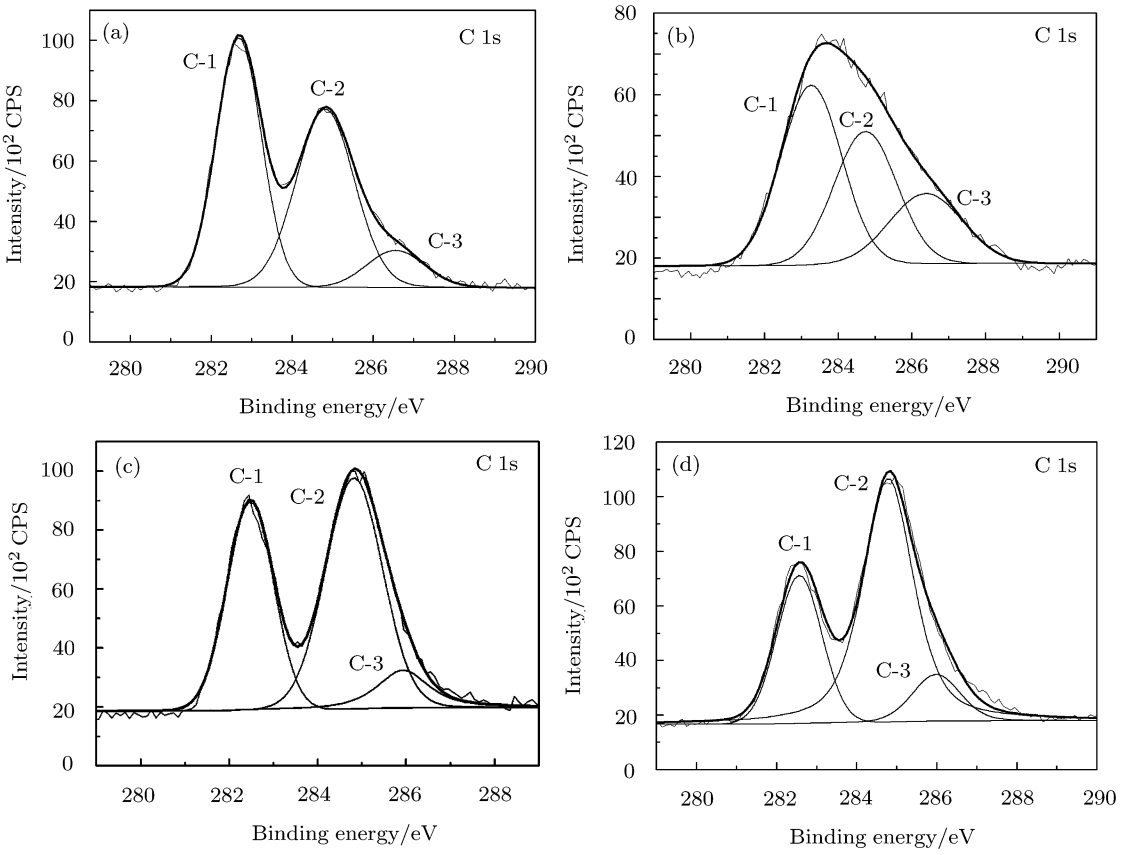


Fig.4. XPS spectra of C 1s, p-type SiC (a) and (b), and n-type SiC (c) and (d) before and after annealing, respectively.

The concentration of C atoms equals that of Si atoms before annealing for both V-implanted p- and n-type SiC samples. The atomic concentration ratio of C to Si decreases dramatically after high temperature annealing for p- and n-type SiC. Si atoms evaporate from the sample and partly redeposit on the surface during annealing, while XPS measurements can only investigate the region near the sample surface. As a result, XPS measurements reveal the increasing of Si concentration. In particular, a higher concentration ratio of Si to C is obtained in an n-type SiC after annealing, indicating the degree of roughness in the n-type sample is more than that in a p-type sample, which can be observed in Figs.2(c) and 2(d).

Capano *et al* have assumed that Si species like Si, Si_2C, SiC_2, etc redeposit on the wafer surface during annealing,[11] but they did not perform any measurements. To investigate the re-deposition species, the surface level spectra of C 1s and Si 2p are measured for V-implanted 4H-SiC samples before and after annealing. The C 1s core-level spectra of V-implanted p- and n-type SiC samples are shown in Figs. 4(a), 4(b) and 4(c), 4(d), respectively. The C 1s surface level spectrum of un-annealed samples indicates the existence of three different peaks for p- and n-type SiC separately as shown in Figs.4(a) and 4(c). The C-1 peak at a binding energy of 282.7 eV corresponds to C-Si bonds from the SiC samples.[20] Two peaks C-2 (284.8 eV) and C-3 (286.0 eV) are related to C–C bonds and C–O bonds, respectively.[21] High temperature annealing results in the decrease of C-1 peaks for p- and n-type samples as shown in Figs.4(b) and 4(d), respectively, which might be due to the evaporation of Si from Si–C bonds during annealing. In particular, C species like Si_2C and SiC_2 are not observed after annealing for p- and n-type samples, respectively. The results differ from the assumed ones in Ref.[11].

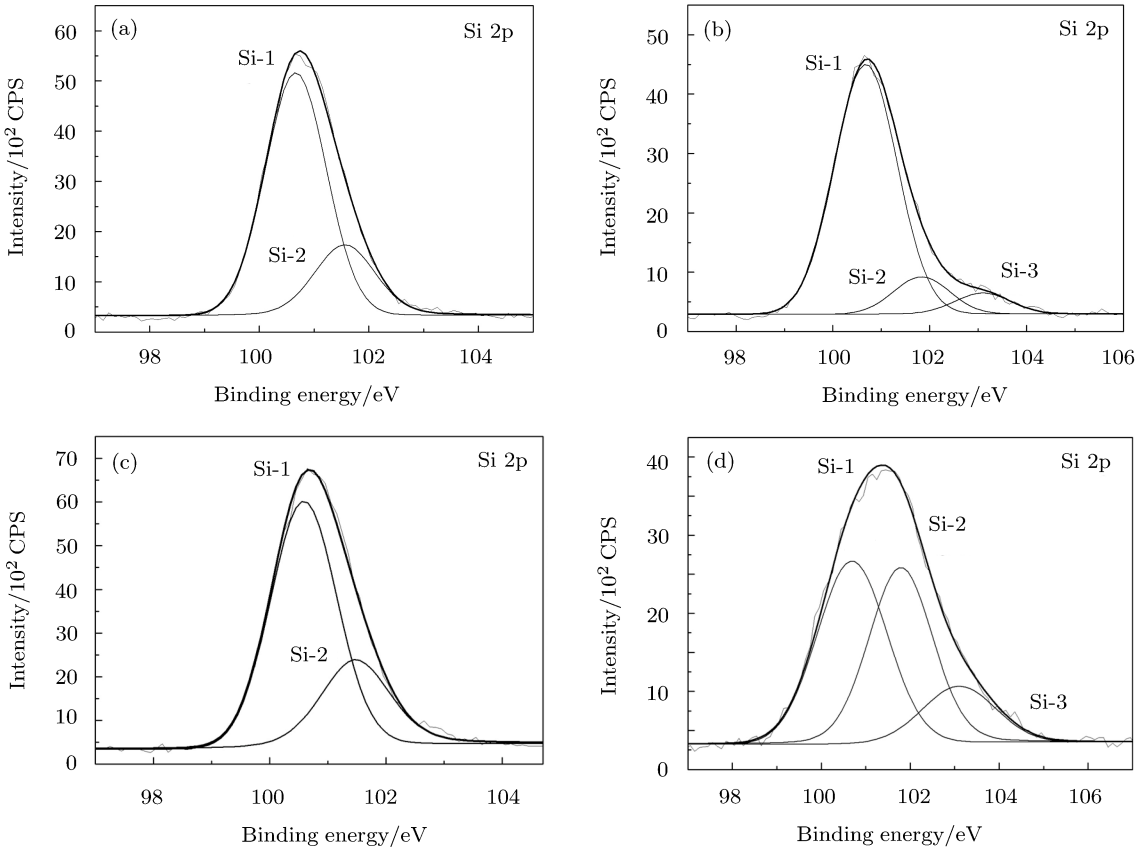


Fig.5. XPS spectra of Si 2p (a), p-type SiC (b) and n-type SiC (c) and (d) before and after annealing, respectively.

Figure 5 shows the XPS spectrum of Si 2p for p- and n-type SiC samples. Figures 5(a) and 5(c) show the Si 2p core-level spectra of p- and n-type SiC samples before annealing respectively. The Si 2p spectra of p- and n-type SiC samples before annealing can be fitted to two Gaussian peaks which are labelled as Si-1 (100.5 eV) and Si-2 (101.7 eV). Si-1 and Si-2 are corresponding to the binding energies of the Si-C bonds[21]

and the Si–O bonds,[22] respectively. The sample annealing at 1650 °C dramatically modifies the Si 2p spectrum (see Figs.5(b) and 5(d)) for p- and n-type SiC, respectively, as a new peak appears at 103.2 eV named Si-3. The existence of Si-3 peak indicates the formation of SiO_2 on the surface after annealing for p- and n-type samples, separately.[23] In addition, the decrease of Si-1 peaks in both annealed p- and n-type samples reveals the evaporation of Si from the SiC during annealing.

4. Conclusions

The diffusion behaviours of V-implanted p- and n-type 4H-SiC are investigated by SIMS. Significant redistributions of V are not found after 1650 °C annealing for p- and n-type samples, respectively. A little higher degree of out-diffusion towards the surface is observed in n-type samples. However, the surface pile-up is not pronounced, which indicates the insignificant out-diffusion behaviour of vanadium in both p- and n-type 4H-SiC samples. V in p-type SiC samples is relatively stable compared with in n-type samples during high temperature annealing. The surface roughness like furrow structures is observed for both p- and n-type samples due to the incongruent evaporation and re-deposition of Si species on the sample surface during annealing. High temperature annealing causes more pronounced degradation of surface in n-type SiC than in p-type SiC. The XPS spectrum analyses of both C 1s and Si 2p demonstrate the evaporation of Si from the samples during annealing for p- and n-type 4H-SiC, respectively. In addition, the existence of Si–O_2 peak indicates the deposition of SiO_2 on the sample surface after high temperature annealing.

Acknowledgments

The authors express their gratitude to Ma Nongnong of Tianjin Electronic Materials Research Institute for performing SIMS measurements and to Li Ying of Xi'an University of Technology for performing XPS measurements.

References

[1] Wang S G, Yang L A, Zhang Y M, Zhang Y M, Zhang Z Y and Yan J F 2003 *Chin. Phys.* **12** 322
[2] Janson M S, Slotte J, Kuznetsov A Y, Saarinen K and Hallen A 2004 *J. Appl. Phys.* **95** 57
[3] Mitchel W C, Mitchell W D, Zvanut M E and Landis G 2004 *Solid State Electron.* **48** 1693
[4] Bickermann M, Weingartner R and Winnacker A 2003 *J. Cryst. Growth* **254** 390
[5] Zvanut M E, Lee W, Mitchel W C, Mitchell W D and Landis G 2006 *Physica* B **376-377** 346
[6] Wang C, Zhang Y M and Zhang Y M 2006 *Chin. J. Semicond.* **27** 1396 (in Chinese)
[7] Wang C, Zhang Y M and Zhang Y M *Chin. Phys.* (to be published)
[8] Edwards A, Dwight D N, Rao M V, Ridgway M C, Kelner G and Papanicolaou N 1997 *J. Appl. Phys.* **82** 4223
[9] Henkel T, Tanaka Y, Kobayashi N, Tanoue H and Hishita S 2001 *Appl. Phys. Lett.* **78** 231
[10] Brauer G, Anwand W, Skorupa W, Brandstetter S and Teichert C 2006 *J. Appl. Phys.* **99** 023523
[11] Capano M A, Ryu S, Melloch M R, Cooper J A, Jr and Buss M R 1998 *J. Electron. Mater.* **27** 370
[12] Ghandi S K 1994 *VLSI Fabrication Principles* (New York: Wiley) Chap.4
[13] Handy E M, Rao M V, Jones K A, Derenge M A, Chi P H, Vispute R D, Venkatesan T, Papanicolaou N A and Mittereder J 1999 *J. Appl. Phys.* **86** 746
[14] Kimoto T, Itoh A and Matsunami H 1997 *Phys. Stat. Sol.* (b) **202** 247
[15] Zhang J, Ellison A and Janzen E 2000 *Mater. Sci. Forum.* **338** 137
[16] Kimoto T, Itoh A and Matsunami H 1997 *J. Appl. Phys.* **81** 3494
[17] Derenge M A, Jones K A, Kirchner K W, Ervin M H, Zheleva T S, Hullavarad S and Vispute R D 2004 *Solid State Electron.* **48** 1867
[18] Guy O J, Doneddu D, Chen L, Jennings M R, Ackland M P, Baylis R, Holton M D, Dunstan P, Wilks S P and Mawby P 2006 *Diamond Relat. Mater.* **15** 1472
[19] Rao S, Bergamini F, Nipoti R and Saddow S E 2006 *Appl. Surf. Sci.* **252** 3837
[20] Li H F, Dimitrijev S, Sweatman D, Harrison H B, Tanner P and Feil B 1999 *J. Appl. Phys.* **86** 4316
[21] Pan J S, Wee T S, Huan H A, Tan H S and Tan K L 1996 *J. Appl. Phys.* **79** 2934
[22] Todi R M, Sundaram K B, Warren A P and Scammon K 2006 *Solid State Electron.* **50** 1189
[23] Larciprete R, Lizzit S, Cepek C, Botti S and Goldoni A 2003 *Surf. Sci.* **532-535** 886